

Attraction centers and \mathcal{PT} -symmetric delta-functional dipoles in critical and supercritical self-focusing media

Li Wang^{1,2}, Boris A. Malomed³, and Zhenya Yan^{1,2,*}

¹*Key Lab of Mathematics Mechanization, Academy of Mathematics and Systems Science, Chinese Academy of Sciences, Beijing 100190, China*

²*School of Mathematical Sciences, University of Chinese Academy of Sciences, Beijing 100049, China*

³*Department of Physical Electronics, School of Electrical Engineering, Faculty of Engineering, and Center for Light-Matter Interaction, Tel Aviv University, Tel Aviv, 59978, Israel*

We introduce a model based on the one-dimensional nonlinear Schrödinger equation (NLSE) with the critical (quintic) or supercritical self-focusing nonlinearity. We demonstrate that a family of solitons, which are unstable in this setting against the critical or supercritical collapse, is stabilized by pinning to an attractive defect, that may also include a parity-time (\mathcal{PT})-symmetric gain-loss component. The model can be realized as a planar waveguide in nonlinear optics, and in a super-Tonks-Girardeau bosonic gas. For the attractive defect with the delta-functional profile, a full family of the pinned solitons is found in an exact analytical form. In the absence of the gain-loss term, the solitons' stability is investigated in an analytical form too, by means of the Vakhitov-Kokolov criterion; in the presence of the \mathcal{PT} -balanced gain and loss, the stability is explored by means of numerical methods. In particular, the entire family of pinned solitons is stable in the quintic (critical) medium if the gain-loss term is absent. A stability region for the pinned solitons persists in the model with an arbitrarily high power of the self-focusing nonlinearity. A weak gain-loss component gives rise to intricate alternations of stability and instability in the system's parameter plane. Those solitons which are unstable under the action of the supercritical self-attraction are destroyed by the collapse. On the other hand, if the self-attraction-driven instability is weak and the gain-loss term is present, unstable solitons spontaneously transform into localized breathers, while the collapse does not occur. The same outcome may be caused by a combination of the critical nonlinearity with the gain and loss. Instability of the solitons is also possible when the \mathcal{PT} -symmetric gain-loss term is added to the subcritical nonlinearity. The system with self-repulsive nonlinearity is briefly considered too, producing completely stable families of pinned localized states.

I. INTRODUCTION AND THE MODEL

It is well established that non-Hermitian Hamiltonians, subject to the constraint of the parity-time (\mathcal{PT}) symmetry, may satisfy the fundamental condition of the reality of energy spectra, hence they may be physically relevant objects [1]-[5]. A single-particle \mathcal{PT} -symmetric Hamiltonian usually contains a complex potential,

$$U(\mathbf{r}) \equiv V(\mathbf{r}) + iW(\mathbf{r}), \quad (1)$$

whose real $V(\mathbf{r})$ and imaginary $W(\mathbf{r})$ parts are, respectively, even and odd functions of coordinates, i.e.,

$$U^*(\mathbf{r}) = U(-\mathbf{r}), \quad (2)$$

where the asterisk stands for the complex conjugate. Usually, the energy spectrum generated by the \mathcal{PT} -symmetric potential remains real below a threshold value of the amplitude of its imaginary part, $W(\mathbf{r})$ in Eq. (1), above which the \mathcal{PT} symmetry breaks down [6, 7]. Nevertheless, examples of systems with unbreakable \mathcal{PT} symmetry are known too [8]. In fact, the linearized version

of the model introduced in the present work also avoids the breakdown, see Eqs. (18) and (19) below.

While the \mathcal{PT} symmetry was not experimentally implemented in quantum systems (and it was argued that it does not hold in the framework of the quantum field theory [11]), the possibility to realize the \mathcal{PT} symmetry in classical photonic media with mutually balanced spatially separated gain and loss elements was elaborated both theoretically [12]-[44] and experimentally [45]-[50]. In addition to that, the same concept can be realized in optomechanics [51], acoustics [52, 53], magnetism [54], and Bose-Einstein condensates [55-57].

Being a linear feature, the \mathcal{PT} symmetry often occurs in combination with the Kerr nonlinearity of optical media in which it is implemented. The respective model amounts to the nonlinear Schrödinger equation (NLSE) with a complex potential which is subject to condition (2). The NLSE gives rise to \mathcal{PT} -symmetric solitons, which were a subject of intensive theoretical work, see, e.g., original papers [14], [20]-[38], [43, 44, 55, 58], and reviews [59, 60]. The existence of \mathcal{PT} -symmetric solitons was also experimentally demonstrated in optical lattices [48]. Although \mathcal{PT} -symmetric media are, as a matter of fact, dissipative ones, solitons in these media appear in continuous families, which is typical for conser-

*Electronic address: zyyan@mmlrc.iss.ac.cn

vative models [61, 62]. It is relevant to stress that \mathcal{PT} -symmetric solitons lose their stability at a critical value of the strength of the gain-loss terms which is smaller than the above-mentioned threshold value, above which the \mathcal{PT} symmetry breaks down in the given system. Between these values, the solitons still exist, but they are unstable [20, 21, 23, 28].

A specific form of the one-dimensional (1D) \mathcal{PT} -symmetric potential (1) is represented by a delta-functional *dipole*, namely,

$$U(x) = -[\varepsilon\delta(x) + i\gamma\delta'(x)] \quad (3)$$

$[\delta'(x)$ stands for the first-order derivative of the delta-function], which was considered in various contexts (including, naturally, a regularized version of the delta-function) [56]-[67]. In particular, an advantage offered by potential (3) is that it allows one to construct exact solutions for solitons pinned to the \mathcal{PT} -symmetric defect embedded in a spatially uniform nonlinear medium [56, 63], although the stability of such states, which is a crucially important issue in the context of \mathcal{PT} symmetry, was addressed by means of numerical methods. Actually, models of this type were previously elaborated only for embedding media with the cubic self-focusing or defocusing nonlinearity. While it indeed represents the most common type of the self-interaction in photonics and other settings which admit the realization of the \mathcal{PT} symmetry, higher-order nonlinearities also occur in optics. In particular, it was experimentally demonstrated that combinations of cubic, quintic, and septimal terms in the optical response of colloidal waveguides can be efficiently engineered by adjusting the size and density of metallic nanoparticles in the colloidal suspension [68, 69]. This technique makes it possible to create an optical medium with a nearly pure quintic or septimal nonlinearity of either sign. On the other hand, a 1D NLSE with the quintic self-attraction is an approximate model of the super-Tonks-Girardeau state, i.e., a quantum gas of strongly interacting bosons in a highly excited state [70]. The attraction center in the bosonic gas can be implemented, as usual, by means of a tightly focused red-detuned laser beam. The consideration of these possibilities is relevant, in particular, because the quintic self-focusing in 1D gives rise to the *critical collapse* and one-dimensional solitons of the *Townes type* [71], suggesting one to look for possibilities to stabilize such solitons, which are unstable in uniform media [72, 73].

The objective of the present work is to consider solitons pinned to the \mathcal{PT} -symmetric defect (3), embedded in the 1D uniform medium with general self-focusing nonlinearity, of power $2\sigma + 1$ with $\sigma > 0$ ($\sigma = 1/2, 1, \text{ and } 2$ correspond, respectively, to the quadratic, cubic, and

critical quintic self-focusing nonlinearities), the respective scaled NLSE for the wave amplitude ψ taking the form of

$$i\psi_z = -\frac{1}{2}\psi_{xx} - |\psi|^{2\sigma}\psi - [\varepsilon\delta(x) + i\gamma\delta'(x)]\psi, \quad (4)$$

where z and x are the propagation distance and transverse coordinate, in terms of the underlying optical planar waveguide, the nonlinearity coefficient is normalized to be +1 (which implies self-focusing), ψ_{xx} represents the paraxial diffraction, and $\varepsilon > 0$ accounts for the attraction strength of the defect (it can be realized by means of the available technique [74], implanting resonant dopants inducing a high refractive index doping in a narrow stripe of the waveguide along the z axis), while its gain-loss component is accounted for by coefficient $\gamma \geq 0$. The latter ingredient of the model can be implemented, also by means of the doping technique, as parallel narrow amplifying and absorbing stripes, separated by a small distance, the respective transverse sizes being on the order of one or few wavelengths of the light beam, while the use of the paraxial propagation equation (4) implies that the transverse size of the beam is much larger than the wavelength, therefore the δ -functions and its derivative offer a natural approximation in this case. The above-mentioned model of the super-Tonks-Girardeau gas may be approximated by Eq. (4) with z replaced by scaled time, t , the quintic self-attraction ($\sigma = 2$), and $\gamma = 0$. The remaining scaling invariance of Eq. (4) allows one to fix $\varepsilon \equiv 1$, replacing the original variables by

$$\tilde{\psi} = \varepsilon^{1/\sigma}\psi, \quad \tilde{z} = \varepsilon^2 z, \quad \tilde{x} \equiv \varepsilon x. \quad (5)$$

This rescaling does not affect γ .

The analysis reported below includes the case of the attraction center in the conservative medium, i.e., $\gamma = 0$, which was previously studied only for the linear and cubic embedding media ($\sigma = 0$ or 1). The present model with $\gamma = 0$ and higher-order nonlinearity, $\sigma > 1$, including the above-mentioned critical (quintic) case, $\sigma = 2$, and *supercritical* one, $\sigma > 2$, makes it possible to construct a full family of exact solutions for solitons pinned to the attractive defect, and predict their stability in an analytical form, by means of the Vakhitov-Kolokolov (VK) criterion, which applies to a broad class of conservative models with self-attraction [73, 75–78] (its generalization for solitons in self-repulsive media, in the form of the *anti-VK criterion*, is known too [79]). Analytical solutions in the form of a family of pinned solitons are also obtained for the \mathcal{PT} -symmetric defect, with $\gamma > 0$, although their stability is investigated by means of a numerically implemented method, with the delta-function replaced, as usual, by its regularized version, see Eq. (39) below.

The rest of the paper is arranged as follows. The general theory and analytical results, including the exact solutions for the delta-functional defect, application of the VK criterion for the stability analysis, and also a brief summary of results for the model with the self-repulsive nonlinearity, are presented in Section II. Numerical findings, including solution of the stability problem through the computation of eigenvalues for small perturbations, and simulations of the evolution of unstable solitons, are reported in Section III. The paper is concluded by Section IV.

II. GENERAL THEORY AND ANALYTICAL RESULTS

A. Stationary states

Stationary localized states with propagation constant $k > 0$ are looked for as solutions to Eq. (4) in the form of

$$\psi(x, z) = e^{ikz} \phi(x), \quad (6)$$

with complex function $\phi(x)$ satisfying the ordinary differential equation with the singular \mathcal{PT} -symmetric potential,

$$-k\phi + \frac{1}{2} \frac{d^2\phi}{dx^2} + |\phi|^{2\sigma}\phi + [\delta(x) + i\gamma\delta'(x)]\phi = 0 \quad (7)$$

[recall $\varepsilon \equiv 1$ is fixed in Eq. (4) by the rescaling (5)]. The complex function $\phi(x)$ in Eq. (7) can be rewritten as [30]

$$\phi(x) = \varphi(x) \exp \left[i \int_{-\infty}^x v(x') dx' \right]$$

with real amplitude $\varphi(x)$ and local wavenumber $v(x)$ satisfying coupled nonlinear ordinary differential equations:

$$\begin{aligned} \varphi''_{xx} + 2\varphi^{2\sigma+1} + [2\delta(x) - v^2 - 2k]\varphi, \\ (\varphi^2 v)'_x = -2\gamma\delta'\varphi^2. \end{aligned} \quad (8)$$

Stability of the stationary states is explored by considering their perturbed version,

$$\psi(x, z) = \left\{ \phi(x) + \eta \left[F(x)e^{i\omega z} + G^*(x)e^{-i\omega^* z} \right] \right\} e^{ikz}, \quad (9)$$

where η is an amplitude of the infinitesimal perturbation with a (generally, complex) eigenvalue, ω , and components $F(x)$ and $G(x)$, which satisfy the matrix equation, produced by the substitution of ansatz (9) and linearization:

$$\begin{pmatrix} \hat{L}_1 & \hat{L}_2 \\ -\hat{L}_2^* & -\hat{L}_1^* \end{pmatrix} \begin{pmatrix} F(x) \\ G(x) \end{pmatrix} = \omega \begin{pmatrix} F(x) \\ G(x) \end{pmatrix}. \quad (10)$$

Here $*$ stands for the complex conjugate, and the constituent operators are

$$\begin{aligned} \hat{L}_1 &= \frac{1}{2} \partial_x^2 + \delta(x) + i\gamma\delta'(x) + (\sigma + 1) |\phi|^{2\sigma} - k, \\ \hat{L}_2 &= \sigma |\phi|^{2(\sigma-1)} \phi^2. \end{aligned} \quad (11)$$

The generic stationary states are stable if all the corresponding eigenvalues ω have zero imaginary parts (the above-mentioned Townes' solitons, that are actually degenerate states, feature a specific subexponentially growing instability, which is accounted for by additional zero eigenvalues).

B. Exact solutions and the Vakhitov-Kokolov stability criterion

In the conservative version of the model, with $\gamma = 0$, an exact real solution to Eq. (7), which may be considered as a soliton pinned to the attractive defect, can be readily obtained:

$$\phi_{\gamma=0}(x) = \left\{ \sqrt{k(\sigma+1)} \operatorname{sech} \left[\sigma\sqrt{2k}(|x| + \xi) \right] \right\}^{1/\sigma}, \quad (12)$$

with real parameter $\xi > 0$ determined by equation

$$\tanh \left(\sigma\sqrt{2k}\xi \right) = \frac{1}{\sqrt{2k}}, \quad (13)$$

i.e.,

$$\xi = \left(2\sigma\sqrt{2k} \right)^{-1} \ln \left(\frac{\sqrt{2k} + 1}{\sqrt{2k} - 1} \right). \quad (14)$$

The squared amplitude of the pinned soliton is

$$A^2(\sigma, k) \equiv \phi_{\gamma=0}^2(x=0) = [(1+\sigma)(k-1/2)]^{1/\sigma}. \quad (15)$$

It follows from Eq. (15) that the solutions exist with the propagation constant exceeding a cutoff value,

$$k > k_{\text{cutoff}} \equiv 1/2, \quad (16)$$

as the amplitude vanishes at $k \rightarrow 1/2$.

Further, a family of exact localized \mathcal{PT} -symmetric solutions to Eq. (7) can also be found in the presence of the gain-loss term, i.e., for $\gamma > 0$, similar to how it was done in Ref. [63] for the cubic nonlinearity ($\sigma = 1$):

$$\begin{aligned} \phi_{\gamma>0}(x) &= \phi_{\gamma=0}(x) \exp \left[-i \operatorname{sgn}(x) \tan^{-1}(\gamma) \right] \\ &\equiv \phi_{\gamma=0}(x) \frac{1 - i\gamma \operatorname{sgn}(x)}{\sqrt{1 + \gamma^2}}, \end{aligned} \quad (17)$$

where $\phi_{\gamma=0}(x)$ is the solution for $\gamma = 0$, as given by Eqs. (12) and (13). The jump in the phase in expression (17) is produced by the singular term $-i\gamma\delta'(x)$ in complex potential (3).

Note that the exact localized solution for the linearized system, with nonlinear term $|\phi|^{2\sigma}\phi$ dropped in Eq. (7), is given by Eqs. (12) and (17) with $\xi \rightarrow \infty$. This solution exists for the single value of the propagation constant, $k = 1/2$ [cf. Eq. (16)],

$$\phi_{k=1/2, \gamma > 0}^{(\text{linear})}(x) = \phi_0 \exp[-|x| - i \operatorname{sgn}(x) \tan^{-1}(\gamma)], \quad (18)$$

where ϕ_0 is an arbitrary constant. In addition to this localized mode existing at the single positive value of k , the linearized system supports a continuous spectrum of delocalized modes with $k < 0$:

$$\phi_{k < 0, \gamma > 0}^{(\text{linear})}(x) = \phi_0 \sin \left[\sqrt{-2k} |x| - \tan^{-1}(\sqrt{-2k}) \right] \times \exp[-i \operatorname{sgn}(x) \tan^{-1}(\gamma)]. \quad (19)$$

Solutions (18) and (19) exist at all values of the gain-loss strength γ , i.e., unlike the above-mentioned generic situation, in the present linearized model the \mathcal{PT} symmetry does not suffer the breakdown with the increase of γ .

A fundamental characteristic of the family of localized states is its norm (alias the integral power, in terms of spatial solitons in the optical waveguide), which is given by the same expression for the solutions with $\gamma = 0$ and $\gamma > 0$:

$$\begin{aligned} N(\sigma, k) &\equiv \int_{-\infty}^{+\infty} |\phi_{\gamma=0}(x)|^2 dx \\ &= \int_{-\infty}^{+\infty} |\phi_{\gamma>0}(x)|^2 dx \\ &= \sqrt{2} \frac{(\sigma+1)^{1/\sigma}}{\sigma} k^{1/\sigma-1/2} \\ &\quad \times \int_0^\infty \left[\operatorname{sech} \left(y + \frac{1}{2} \ln \left(\frac{\sqrt{2k}+1}{\sqrt{2k}-1} \right) \right) \right]^{2/\sigma} dy, \quad (20) \end{aligned}$$

In the limit of $k \rightarrow 1/2$, Eq. (20) demonstrates that the norm vanishes as

$$N(\sigma, k) \approx \left[(1+\sigma) (\sqrt{2k}-1) \right]^{1/\sigma}. \quad (21)$$

According to the VK criterion [73, 75–78], the necessary stability condition in the conservative model, with $\gamma = 0$, is $\partial N / \partial k > 0$. In particular, in the case of the usual Kerr nonlinearity ($\sigma = 1$), Eq. (20) takes a very simple form [63],

$$N(\sigma = 1, k) = 2 (\sqrt{2k} - 1), \quad (22)$$

which implies an evident result, that the pinned solitons are VK-stable modes in the cubic medium. Similar to this result, the norm of the pinned solitons diverges, at $k \rightarrow \infty$, for all subcritical nonlinearities, with $\sigma < 2$, as

$$N(\sigma, k) \approx \sqrt{\frac{\pi}{2}} \frac{(\sigma+1)^{1/\sigma}}{\sigma} \frac{\Gamma(1/\sigma)}{\Gamma(1/2+1/\sigma)} k^{1/\sigma-1/2}, \quad (23)$$

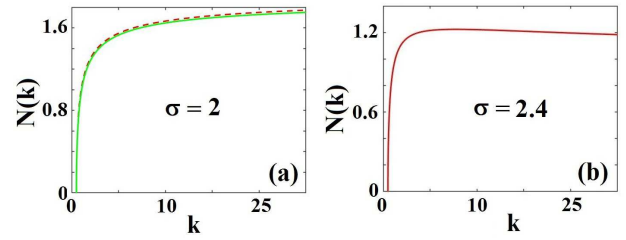


FIG. 1: (Color online). (a) Norm $N(\sigma, k)$ versus parameter k at $\sigma = 2$. The solid green line represents the exact solution corresponding to Eq. (24), while the dotted red line is produced by the numerical solution of Eq. (12) with the delta-function regularized as per Eq. (39). The application of the VK criterion to the $N(\sigma = 2, k)$ dependence suggests that the entire family of the 1D Townes' solitons is *completely stabilized* by pinning to the attractive defect. (b) The approximate dependence $N(\alpha, k)$ given by Eq. (26) with $\sigma = 2.4$.

where Γ is the Gamma-function.

More interesting is the critical case of $\sigma = 2$ (the quintic nonlinearity), which was not considered previously in the combination with the attractive defect. In this case, Eq. (20) yields

$$N(\sigma = 2, k) = \sqrt{\frac{3}{2}} \left[\pi - 2 \tan^{-1} \left(\sqrt{\frac{\sqrt{2k}+1}{\sqrt{2k}-1}} \right) \right], \quad (24)$$

see Fig. 1(a). The uniform medium [with $\varepsilon = 0$, in terms of Eq. (3)] formally corresponds to $k \rightarrow \infty$, which implies the degeneracy of the corresponding family of the 1D Townes' solitons: their norm takes a single value,

$$N_{\text{Townes}} = \sqrt{3/2} (\pi/2) \approx 1.92, \quad (25)$$

which does not depend on the soliton's propagation constant. In terms of the VK criterion, the constant norm formally corresponds to the neutral stability, with $\partial N / \partial k = 0$. However, it is well known that the Townes' solitons are always unstable against the spontaneous onset of the *critical collapse*, although their instability is subexponential, as mentioned above [73] (for this reason, it is not detected by the VK criterion).

In the case of $\gamma = 0$ and $\sigma = 2$, Eq. (24) clearly demonstrates $\partial N / \partial k > 0$ at all values of $k > \frac{1}{2}$ (see Fig. 1), suggesting that the 1D Townes' solitons, which are completely unstable in the free space, are *completely stabilized* by the attractive center, irrespective of its strength. This conjecture was corroborated by the full stability analysis based on the numerical solution of eigenvalue equation (10), as well as by direct simulations of the perturbed evolution of the pinned solitons.

For the slightly supercritical case, with $2 < \sigma \ll 3$, the $N(\sigma, k)$ dependence derived from Eq. (20) can be

approximated by

$$N(\sigma, k) \approx \sqrt{\frac{3}{2}} (2k)^{(2-\sigma)/4} \left[\pi - 2 \tan^{-1} \left(\sqrt{\frac{\sqrt{2k+1}}{\sqrt{2k-1}}} \right) \right]. \quad (26)$$

This dependence satisfies the VK criterion at

$$\frac{1}{2} < k < k_{\text{cr}} \approx \frac{8}{(\pi(\sigma-2))^2}, \quad (27)$$

and does not satisfy it at $k > k_{\text{cr}}$. The approximate dependence (26) attains a maximum at $k = k_{\text{cr}}$, which, in the lowest approximation, turns out to be $N_{\text{max}} = N_{\text{Townes}}$, see Eq. (25). Accordingly, the pinned solitons are expected to be stable in this supercritical case (with $\gamma = 0$, i.e., in the absence of the gain and loss) in the region of $1/2 < k < k_{\text{cr}}$, and to suffer the onset of the *supercritical collapse* (spontaneous blowup) at $k > k_{\text{cr}}$. In particular, for $\sigma = 2.4$ (not very close to $\sigma = 2$, but still relatively close), the dependence given by Eq. (26) is plotted in Fig. 1(b), where $k_{\text{cr}} \approx 7.75$, while approximation (27) yields $k_{\text{cr}} \approx 5.07$ for $\sigma = 2.4$.

Another corollary of Eqs. (26) and (27) is that derivative $\partial N_{\text{max}}/\partial\sigma$ slowly diverges at the border of the supercritical case, i.e., at $\sigma \rightarrow 2$:

$$\frac{\partial N_{\text{max}}}{\partial\sigma} \approx -\sqrt{\frac{3}{2}} \frac{\pi}{4} \ln \left(\frac{1}{\sigma-2} \right). \quad (28)$$

This result agrees with the fact that $N_{\text{max}} = \infty$ at $\sigma < 2$, as it follows from Eq. (23).

Figure 2 displays the dependence $N(\sigma, k)$, numerically calculated as per Eq. (20), for different critical and supercritical values of the nonlinearity power, *viz.*, $\sigma = 2, 2.25, 2.5, 2.75, 3$. While, as said above, in the critical case of $\sigma = 2$ condition $\partial N(\sigma, k)/\partial k > 0$ holds at all $k > \frac{1}{2}$, at each supercritical value, $\sigma > 2$, the $N(\sigma, k)$ dependence indeed features the critical point, k_{cr} , at which the slope, $\partial N/\partial k$, changes its sign, and the norm attains its largest value, $N_{\text{max}} = N(k_{\text{cr}})$ [note that, as follows from Eq. (20), $N(\sigma, k \rightarrow \infty) \sim (2k)^{(1/\sigma-1/2)} \rightarrow 0$, for any $\sigma > 2$]. The prediction of the VK criterion, that, in the case of $\gamma = 0$, the pinned solitons are stable in the region of $1/2 < k < k_{\text{cr}}$, i.e., $0 < N < N_{\text{max}}$, is corroborated by the calculation of the stability eigenvalues via Eq. (10), as well as by direct simulations of perturbed evolutions of the solitons. In particular, the VK-unstable solitons, existing at $k > k_{\text{cr}}$, are indeed destructed by the spontaneous blowup, see Fig. 4(a) below. Thus, the attractive defect provides for the partial stabilization of the solitons in the case of the supercritical nonlinearity, for all values of $\sigma > 2$, while all solitons are strongly unstable in this case in the absence of the defect. Naturally,

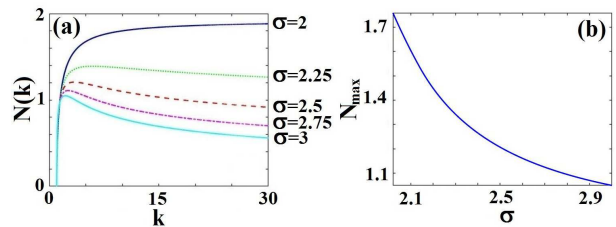


FIG. 2: (Color online). (a) The dependence of norm $N(\sigma, k)$ on propagation constant k , numerically computed as per Eq. (20), for the critical case, with $\sigma = 2$, and the supercritical one, with $\sigma = 2.25, 2.5, 2.75, 3$. (b) The maximum norm of the pinned solitons, attained at the stability-boundary, $k = k_{\text{cr}}$, at which $\partial N/\partial k = 0$, versus σ (in the supercritical interval, $2 < \sigma \leq 3$). In the case of $\gamma = 0$, the pinned solitons are stable in the region of $1/2 < k < k_{\text{cr}}$, which corresponds to $0 < N < N_{\text{max}}$.

Fig. 2(a) demonstrates that the stability region (in both forms of $1/2 < k < k_{\text{cr}}$ and $0 < N < N_{\text{max}}$), maintained by the interplay of the supercritical self-attractive nonlinearity and attraction center, shrinks with the increase of the nonlinearity power, σ . Nevertheless, the stability region persists even at large values of σ . Indeed, if σ is treated as a large parameter, while $k - \frac{1}{2}$ as a small one, Eq. (20) amounts to

$$N(\sigma \gg 1, k) \approx (2k)^{-1/2} (\sqrt{2k} - 1)^{1/\sigma} \quad (29)$$

[cf. Eq. (21)], which yields

$$k_{\text{cr}} - \frac{1}{2} \approx 1/\sigma, \quad \lim_{\sigma \rightarrow \infty} N_{\text{max}} = 1. \quad (30)$$

The limit value of $N_{\text{max}} = 1$, given by Eq. (30), agrees with the numerical results displayed in Figs. 2(b) and 3(d).

Finally, to better understand the physical meaning of the \mathcal{PT} -symmetric stationary state, $\phi_{\gamma>0}(x)$, given by Eq. (17), it is relevant look at its power flux (the Poynting vector), $S(x) = \text{Im}(\phi^*(x) \frac{d}{dx} \phi(x))$. The substitution of Eqs. (7) and (17) yields a singular expression,

$$S(x) = -2\gamma \phi_{\gamma=0}^2(x) \delta(x), \quad (31)$$

A regular characteristic of the transport in the \mathcal{PT} -symmetric pattern is provided by the globally normalized flux,

$$\begin{aligned} \hat{S} &\equiv N^{-1}(\sigma, k) \int_{-\infty}^{+\infty} S(x) dx \\ &= -2\gamma A^2(\sigma, k)/N(\sigma, k) < 0, \end{aligned} \quad (32)$$

where $A(\sigma, k)$ is the amplitude of the pinned soliton, given by Eq. (15). An essential feature of this expression is its sign, which, in comparison with Eq. (4), clearly demonstrates that the power flows, as it should, from the source (gain) towards the sink (loss).

C. Exact solutions with the self-defocusing nonlinearity

It is relevant to briefly consider the model with the self-repulsive uniform nonlinearity, i.e., with Eq. (4) replaced by

$$i\psi_z = -\frac{1}{2}\psi_{xx} + |\psi|^{2\sigma}\psi - [\varepsilon\delta(x) + i\gamma\delta'(x)]\psi. \quad (33)$$

In this case, the exact solution for $\gamma = 0$ is readily found as

$$\phi_{\gamma=0}^{(\text{defoc})}(x) = \left\{ \sqrt{k(\sigma+1)} / \sinh \left[\sigma\sqrt{2k}(|x| + \xi) \right] \right\}^{1/\sigma}, \quad (34)$$

with

$$\xi = \frac{1}{2\sigma\sqrt{2k}} \ln \left(\frac{1 + \sqrt{2k}}{1 - \sqrt{2k}} \right), \quad (35)$$

and the squared amplitude

$$B^2(\sigma, k) \equiv \left[\phi_{\gamma=0}^{(\text{defoc})}(x=0) \right]^2 = [(1 + \sigma)(1/2 - k)]^{1/\sigma}. \quad (36)$$

As it follows from Eq. (36), the existence region for the localized modes pinned to the attractive defect embedded in the defocusing medium is $k < k_{\text{cutoff}} \equiv 1/2$, which is exactly opposite to that in the case of self-focusing, cf. Eq. (16).

In the presence of the gain-loss dipole, which introduces the \mathcal{PT} symmetry, i.e., $\gamma > 0$, the exact solution is generated from the one for $\gamma = 0$ by the same relation (17) which is relevant in the case of self-focusing. As concerns the norm, it takes a simple form in the cubic defocusing medium ($\sigma = 1$),

$$N^{(\text{defoc})}(\sigma = 1, k) = 2 \left(1 - \sqrt{2k} \right) \quad (37)$$

[cf. Eq. (22)]. On the other hand, in the limit case of large σ , the result is

$$N^{(\text{defoc})}(\sigma \gg 1, k) \approx (2k)^{-1/2} \left(1 - \sqrt{2k} \right)^{1/\sigma}, \quad (38)$$

cf. Eq. (29). It can be checked that, as well as it is obvious in Eqs. (37) and (38), the $N(\sigma, k)$ dependence corresponding to the defocusing nonlinearity satisfies the above-mentioned anti-VK criterion, $\partial N / \partial k < 0$ [79], at all values of σ . Accordingly, all the pinned modes are stable, both at $\gamma = 0$ and $\gamma > 0$, similar to the case of the self-defocusing cubic nonlinearity [63].

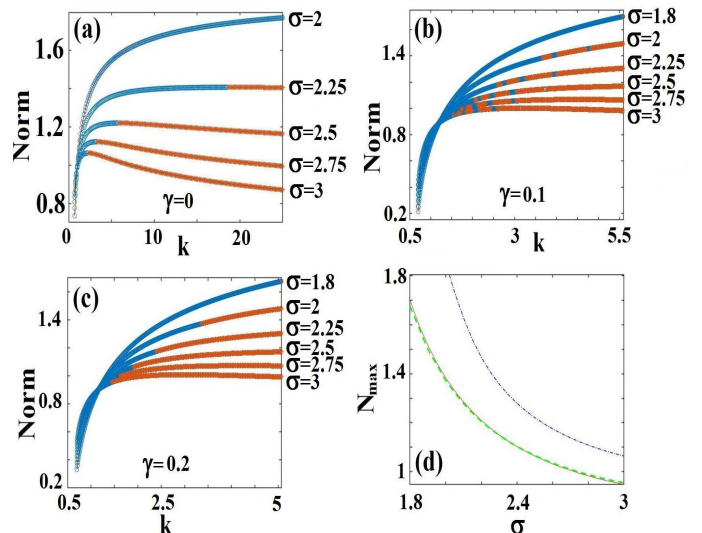


FIG. 3: (Color online). The norm of stable solitons (blue circles) and unstable solitons (red stars) produced by the numerical solution of Eq. (12) with the regularized delta-function (39), for different values of the nonlinearity degree σ and gain-loss coefficient γ : (a) $\gamma = 0$, (b) $\gamma = 0.1$, (c) $\gamma = 0.2$. The stability is identified through the numerical solution of eigenvalue problem (10), using the same regularization. Note the difference in the scales of the horizontal axes between panels (a) and (b,c). The top and bottom curves in panel (d) display stability boundaries in the plane of (σ, N) for $\gamma = 0$ (dash-dotted blue line), 0.1 (solid red line), and 0.2 (dashed green line) (the boundaries for $\gamma = 0.1$ and $\gamma = 0.2$ are practically identical).

III. NUMERICAL SOLUTIONS AND THEIR STABILITY

A. Stationary states and small perturbations

While the model with the ideal delta-functional defect admits exact solutions for all values of σ and γ , as given by Eqs. (12), (14), and (17), their stability in the \mathcal{PT} -symmetric model with $\gamma > 0$ is a nontrivial problem which should be addressed by means of numerical methods. For this purpose, the ideal delta-function is replaced by the well-known Gaussian regularization,

$$\delta(x) \rightarrow \tilde{\delta}(x) = \frac{1}{\sqrt{\pi}a} \exp\left(-\frac{x^2}{a^2}\right), \quad (39)$$

with width a much smaller than a characteristic size of the pinned mode. This condition is secured by fixing $a = 0.03$, which is adopted here. It was checked that taking smaller a does not affect the results in any conspicuous way.

Stationary equation (12) with $\delta(x)$ and $\delta'(x)$ replaced by $\tilde{\delta}(x)$ and $\tilde{\delta}'(x)$ can be efficiently solved by means of the Petviashvili iteration method [80], using the above-

mentioned analytical solution, valid in the limit of the ideal delta-function, as the initial guess. Then, Eqs. (10) and (11), regularized as per substitution (39), are numerically solved to predict the stability boundary. Finally, perturbed evolution of the pinned modes was simulated by means of fourth-order Runge-Kutta time-stepping scheme. A known necessary and sufficient condition for the stability of the direct simulations amounts to an inequality imposed on the time and space steps, $\Delta t/(\Delta x)^2 \leq 2\sqrt{2}/\pi^2$ [78]. As a result, it is concluded that the real numerically generated solutions for $\gamma = 0$, as well as real parts of the complex solutions for $\gamma > 0$, are very close to the analytically predicted counterparts [see Figs. 4(a1,b1,c1,d1,e1)]. A small difference of the imaginary parts in the latter case (hence, of the phase structure of the complex solitons) from the analytical form given by Eq. (17) is explained by the fact that the numerical solution cannot exactly follow the discontinuous shape of the solution produced by Eq. (17).

Figure 3(a) summarizes results for the stability of the pinned solitons, produced by the numerical solution of Eqs. (7) and (10) subject to linearization (39), for the critical and supercritical values of the nonlinearity power, $\sigma = 2$ and 2.25, 2.5, 2.75, 3, in the absence of the gain and loss ($\gamma = 0$). It is seen that the stability precisely follows the VK criterion, and, in the exact agreement with the analytical prediction, the solitons are completely stable for $\sigma = 2$, while the stability region shrinks with the increase of σ in the supercritical case. The respective existence and stability boundary, $N_{\max}(\sigma)$, which is shown by the top curve in Fig. 3(d), is identical to its analytically predicted counterpart, cf. Fig. 2(b).

As it may be expected, the stability pattern becomes more complex in the presence of the gain-and-loss term, i.e., at $\gamma > 0$, see Figs. 3(b) and (c) for $\gamma = 0.1$ and 0.2. It is observed that the VK criterion is no longer sufficient for the stability, in this case. For the relatively large value $\gamma = 0.2$, Fig. 3(c) demonstrates strong shrinkage of the stability region, in comparison with the case of $\gamma = 0$; in particular, the critical nonlinearity, with $\sigma = 2$, keeps the pinned solitons stable only at $N < N_{\max} \approx 1.32$, while, at $\gamma = 0$, the same nonlinearity maintains the stability in the entire existence region of the solitons, up to $N = N_{\text{Townes}}$, see Eq. (25). The numerically found stability boundaries for $\gamma = 0.1$ and 0.2, in the form of $N_{\max}(\sigma)$, are displayed by two bottom curves (which are virtually identical to each other) in Fig. 3(d).

Figure 3(b) features an intricate structure of the stability pattern, with *multiple stability intervals*, at smaller values of the gain-loss coefficient, such as $\gamma = 0.1$. As seen in Fig. 3(d), the lowest stability boundary for

$\gamma = 0.1$ is virtually identical to one for $\gamma = 0.2$. However, the actual number of such boundaries observed in 3(b) is, at least, five. Probably, many more boundaries may be revealed by extremely precise numerical data, and it seems plausible that the exact structure of the stability islands, embedded in the instability area, may be *fractal*, as suggested, in particular, by the fractal alternation of regions of elastic and inelastic collisions between solitons in some nonintegrable conservative models [81–83]. The fractal structure, if any, may strongly depend in values of γ and σ . A rigorous analysis of this challenging problem is beyond the scope of the present work.

In the presence of the gain and loss, the instability occurs even in the subcritical case, i.e., at $\sigma < 2$. While in Figs. 3(b, c) the subcritical branches, corresponding to $\sigma = 1.8$, are completely stable in the displayed range of k , they develop weak instability at essentially larger values of k , where the VK derivative, $\partial N/\partial k \sim k^{1/\sigma-3/2}$ [see Eq. (23)] is very small, hence the effect of the subcriticality is insufficient to suppress the instability induced by the possibility of spontaneous breaking of the \mathcal{PT} symmetry. In particular, for $\sigma = 1.8$ and $\gamma = 0.2$, the pinned soliton is unstable at $k = 20$, see Figs. 4(e2,e3) below.

B. Direct simulations

The predictions for the (in)stability of the pinned solitons, produced by the application of the VK (or anti-VK) criterion to the analytical solutions in the case of $\gamma = 0$, and by the numerical solution of Eq. (10), subject to regularization (39), for the numerically constructed solutions in the case of $\gamma \geq 0$, were verified by direct simulations of perturbed evolutions of the pinned solitons. It has been concluded that all the modes which were predicted to be stable are stable indeed (not shown here in detail, as simulations of the stable evolution do not reveal new features of the dynamics). The predicted instability is also corroborated by the direct simulations, as shown in Fig. 4. In particular, in the case of $\gamma = 0$ the instability, displayed in panel (a2), leads to sudden blowup of the solution, which is a manifestation of the supercritical collapse. The same happens too, but faster, as a result of the interplay of the supercritical self-attraction and gain-loss ($\gamma = 0.2$) term, see panel (b2). Panel (c2) demonstrates that, in the case of large k , when the instability related to the supercriticality is weak, as the derivative, $|\partial N/\partial k|$, which determines the VK criterion, is small, see Figs. 1(b) and 2(a), the interplay of the weak instability and gain-loss terms leads not to a blowup, but to the formation of a robust localized breather with an amplitude

which is essentially smaller than in the original unstable soliton.

Recall that, in the absence of the gain-loss term, all the pinned solitons maintained by the critical nonlinearity, with $\sigma = 2$, are stable. The addition of the sufficiently strong gain and loss [in particular, with $\gamma = 0.2$, as shown in Fig. 4(d2)] may destabilize the solitons in this case. It is observed in the figure that the initial stage of the instability-driven evolution is chaotic, eventually relaxing to a robust breather.

Finally, as it was mentioned above, the presence of the gain-loss term may induce instability in the subcritical case, $\sigma < 2$. Figure 4(e2) demonstrates an example of this instability for $\sigma = 1.8$ and $\gamma = 0.2$, provided that the soliton was created with a large value of the propagation constant (in particular, $k = 20$ in this figure), where, as said above, the stabilizing effect of the subcritical instability is very weak. In this case too, the collapse does not occur (as there is nothing to drive it in the subcritical case), the instability leading to spontaneous transformation of the unstable soliton into a robust breather with an essentially smaller amplitude.

As seen from Fig. 3, the stability region of the \mathcal{PT} -symmetric solitons shrinks with the increase of both the nonlinearity power, σ , and gain-loss coefficient, γ . Systematically collecting numerical data, we conclude that, at a fixed value of σ , all the solitons become unstable at $\gamma > \gamma_{\max}(\sigma)$, and, at a fixed value of γ , the same happens at $\sigma > \sigma_{\max}(\gamma)$. As concerns value N_{\max} of the norm at which the stability ends, it essentially depends on σ and very weakly depends on γ , as shown by the stability boundaries in the (σ, N) plane for $\gamma = 0.1$ and 0.2 in Fig. 3(d), which are virtually identical for both these values of γ . For a fixed value of the norm, $N < N_{\max}$, the dependence of the stability border of γ is very weak too.

IV. CONCLUSIONS AND DISCUSSIONS

The objective of this work is to introduce settings in which intrinsically unstable solitons in 1D media modelled by the NLSE with the critical ($\sigma = 2$) and supercritical ($\sigma > 2$) self-attractive nonlinearity may be stabilized by pinning to an attractive defect, including its \mathcal{PT} -symmetric version with strength γ of the gain-loss com-

ponent. The settings represent a planar nonlinear-optical waveguide, or a super-Tonks-Girardeau gas. A remarkable fact is that full families of the pinned solitons can be found in the analytical form for the delta-functional defect, and, in the absence of the gain-loss term, their stability too admits analytical investigation, by means of the VK criterion. In particular, a stability interval exists for arbitrarily high values of the nonlinearity power σ . In the presence of the gain and loss, the stability of the \mathcal{PT} -symmetric soliton families and the evolution of unstable solitons were investigated by means of numerical methods, revealing a nontrivial stability area in the (σ, γ) plane. For relatively small values of γ , the structure of the stability area is intricate, featuring multiple stability boundaries (which may presumably form a fractal). If the instability driven by the supercritical nonlinearity is strong enough, unstable solitons are destroyed by the collapse, both in the absence and presence of the gain-loss term. On the other hand, if the supercritical instability is weak, it does not lead, in the combination with the balanced gain and loss ($\gamma > 0$), to the collapse; instead, it spontaneously replaces unstable solitons by robust localized breathers. The same happens to those solitons which are unstable under the action of the critical nonlinearity combined with the gain-loss term. Instability is also possible if the gain and loss are added to the subcritical instability, which is close to the critical case. In the latter case, breathers emerge as well. The model with the self-repulsion was briefly considered too, with the conclusion that the localized modes pinned to the attractive defect are completely stable in that case.

A challenging direction for the extension of the present analysis is to develop it in a two-dimensional model, which may also be realized in nonlinear optics, using a bulk waveguide, with the local defect represented by an elongated core embedded in the medium.

Acknowledgments

The present work was supported in the framework of NSFC (China) under grants Nos. 11571346, 11731014, and 61621003, Interdisciplinary Innovation Team of Chinese Academy of Sciences, and the Chinese Academy of Sciences President's International Initiative (PIFI).

[1] C. M. Bender and S. Boettcher, Real spectra in non-Hermitian Hamiltonians having \mathcal{PT} symmetry. *Phys. Rev. Lett.* **80**, 5243-5246 (1998).

[2] P. Dorey, C. Dunning, and R. Tateo, Spectral equivalences, Bethe ansatz equations, and reality properties in \mathcal{PT} -symmetric quantum mechanics, *J. Phys. A: Math.*

- Gen. **34**, 5679-5704 (2001).
- [3] C. M. Bender, D. C. Brody, and H. F. Jones, Complex extension of quantum mechanics, *Phys. Rev. Lett.* **89**, 270401 (2002).
- [4] C. M. Bender, Making sense of non-Hermitian Hamiltonians, *Rep. Prog. Phys.* **70**, 947-1018 (2007).
- [5] N. Moiseyev, *Non-Hermitian Quantum Mechanics*, (Cambridge University Press, 2011).
- [6] J. Yang, Symmetry breaking of solitons in one-dimensional parity-time-symmetric optical potentials, *Opt. Lett.* **39**, 5547-5550 (2014).
- [7] S. Nixon and J. Yang, Nonlinear wave dynamics near phase transition in \mathcal{PT} -symmetric localized potentials, *Physica D* **331**, 48-57 (2016).
- [8] V. Lutsky, E. Luz, E. Granot, and B. A. Malomed, Making the \mathcal{PT} symmetry unbreakable, in: *Parity-time Symmetry and Its Applications*, pp. 443-464, ed. by D. Christodoulides and J. Yang (Springer, Singapore, 2018).
- [9] K. G. Makris, R. El-Ganainy, D. N. Christodoulides, and Z. H. Musslimani \mathcal{PT} symmetric periodic optical potentials, *Int. J. Theor. Phys.* **50**, 1019-1041 (2011).
- [10] H. Ramezani, T. Kottos, R. El-Ganainy, and D. N. Christodoulides, Unidirectional nonlinear \mathcal{PT} -symmetric optical structures, *Phys. Rev. A* **82**, 043803 (2010).
- [11] S. Scheel and A. Szameit, \mathcal{PT} -symmetric photonic quantum systems with gain and loss do not exist, *EPL* **122**, 34001 (2018).
- [12] A. Ruschhaupt, F. Delgado, and J. G. Muga, Physical realization of \mathcal{PT} -symmetric potential scattering in a planar slab waveguide, *J. Phys. A: Math. Gen.* **38**, L171-L176 (2005).
- [13] R. El-Ganainy, K. G. Makris, D. N. Christodoulides, and Z. H. Musslimani, Theory of coupled optical \mathcal{PT} -symmetric structures, *Opt. Lett.* **32**, 2632-2634 (2007).
- [14] Z. H. Musslimani, K. G. Makris, R. El-Ganainy, and D. N. Christodoulides, Optical solitons in \mathcal{PT} periodic potentials, *Phys. Rev. Lett.* **100**, 030402 (2008).
- [15] M. V. Berry, Optical lattices with \mathcal{PT} -symmetry are not transparent, *J. Phys. A: Math. Theor.* **41**, 244007 (2008).
- [16] S. Klaiman, U. Günther, and N. Moiseyev, Visualization of branch points in \mathcal{PT} -symmetric waveguides, *Phys. Rev. Lett.* **101**, 080402 (2008).
- [17] O. Bendix, R. Fleischmann, T. Kottos, and B. Shapiro, Exponentially fragile \mathcal{PT} symmetry in lattices with localized eigenmodes, *Phys. Rev. Lett.* **103**, 030402 (2009).
- [18] S. Longhi, Bloch oscillations in complex crystals with \mathcal{PT} symmetry, *Phys. Rev. Lett.* **103**, 123601 (2009).
- [19] K. G. Makris, R. El-Ganainy, D. N. Christodoulides, and Z. H. Musslimani, \mathcal{PT} -symmetric optical lattices, *Phys. Rev. A* **81**, 063807 (2010).
- [20] D. A. Zezyulin, Y. V. Kartashov, and V. V. Konotop, Stability of solitons in \mathcal{PT} -symmetric nonlinear potentials, *EPL* **96**, 64003 (2011).
- [21] R. Driben and B. A. Malomed, Stability of solitons in parity-time-symmetric couplers, *Opt. Lett.* **36**, 4323-4325 (2011).
- [22] K. G. Makris, R. El-Ganainy, D. N. Christodoulides, and Z. H. Musslimani, \mathcal{PT} -Symmetric periodic optical potentials, *Int. J. Theor. Phys.* **50**, 1019 (2011).
- [23] N. V. Alexeeva, I. V. Barashenkov, A. A. Sukhorukov, and Y. S. Kivshar, Optical solitons in \mathcal{PT} -symmetric nonlinear couplers with gain and loss, *Phys. Rev. A* **85**, 063837 (2012).
- [24] M.-A. Miri, A. B. Aceves, T. Kottos, V. Kovanis, and D. N. Christodoulides, Bragg solitons in nonlinear \mathcal{PT} -symmetric periodic potentials, *Phys. Rev. A* **86**, 033801 (2012).
- [25] Z. Yan, Complex \mathcal{PT} -symmetric nonlinear Schrödinger equation and Burgers equation, *Phil. Trans. R. Soc. London, Ser. A* **371**, 20120059 (2013).
- [26] Z. Chen, J. Liu, S. Fu, Y. Li, and B. A. Malomed, Discrete solitons and vortices on two-dimensional lattices of \mathcal{PT} -symmetric couplers, *Opt. Exp.* **22**, 29679-29692 (2014).
- [27] Z. Yan, Z. Wen, and C. Hang, Spatial solitons and stability in self-focusing and defocusing Kerr nonlinear media with generalized parity-time-symmetric Scarff-II potentials, *Phys. Rev. E* **92**, 022913 (2015).
- [28] S. Nixon, L. Ge, and J. Yang, Stability analysis for solitons in \mathcal{PT} -symmetric optical lattices, *Phys. Rev. A* **85**, 023822 (2012).
- [29] J. D'Ambroise, P. G. Kevrekidis, and B. A. Malomed, Staggered parity-time-symmetric ladders with cubic nonlinearity, *Phys. Rev. E* **91**, 033207 (2015).
- [30] Z. Yan, Z. Wen, and V. V. Konotop, Solitons in a nonlinear Schrödinger equation with \mathcal{PT} -symmetric potentials and inhomogeneous nonlinearity: Stability and excitation of nonlinear modes, *Phys. Rev. A* **92**, 023821 (2015).
- [31] Z. Yan, Y. Chen, and Z. Wen, On stable solitons and interactions of the generalized Gross-Pitaevskii equation with \mathcal{PT} - and non- \mathcal{PT} -symmetric potentials, *Chaos* **26**, 083109 (2016).
- [32] Y. Chen and Z. Yan, Solitonic dynamics and excitations of the nonlinear Schrödinger equation with third-order dispersion in non-Hermitian \mathcal{PT} -symmetric potentials, *Sci. Rep.* **6**, 23478 (2016).
- [33] Y. Chen, Z. Yan, D. Mihalache, and B. A. Malomed, Families of stable solitons and excitations in the \mathcal{PT} -symmetric nonlinear Schrödinger equations with position-dependent effective masses, *Sci. Rep.* **7**, 1257 (2017).
- [34] Y. Chen and Z. Yan, Stable parity-time-symmetric nonlinear modes and excitations in a derivative nonlinear Schrödinger equation, *Phys. Rev. E* **95**, 012205 (2017).
- [35] Z. Yan and Y. Chen, The nonlinear Schrödinger equation with generalized nonlinearities and \mathcal{PT} -symmetric potentials: Stable solitons, interactions, and excitations, *Chaos* **27**, 073114 (2017).
- [36] Z. Wen and Z. Yan, Solitons and their stability in the nonlocal nonlinear Schrödinger equation with \mathcal{PT} -symmetric potentials, *Chaos* **27**, 053105 (2017).
- [37] N. V. Alexeeva, I. V. Barashenkov, and Y. S. Kivshar, Solitons in \mathcal{PT} -symmetric ladders of optical waveguides, *New J. Phys.* **19**, 113032 (2017).
- [38] E. Luz, V. Lutsky, E. Granot, and B. A. Malomed, Robust \mathcal{PT} symmetry of two-dimensional fundamental and vortex solitons supported by spatially modulated nonlinearity, *Sci. Rep.* **9**, 4483 (2019).
- [39] Y. Kominis, T. Bountis, and S. Flach, Stability through asymmetry: Modulationally stable nonlinear supermodes of asymmetric non-Hermitian optical couplers, *Phys. Rev.* **95**, 063832 (2017).
- [40] Y. Chen, Z. Yan, and X. Li, One- and two-dimensional gap solitons and dynamics in the \mathcal{PT} -symmetric lattice potential and spatially-periodic momentum modulation, *Commun. Nonlinear Sci. Numer. Simul.* **55**, 287 (2018).
- [41] Y. Chen, Z. Yan, and W. Liu, Impact of near- \mathcal{PT} symmetry on exciting solitons and interactions based on a

- complex Ginzburg-Landau model, *Opt. Exp.* **26**, 33022 (2018).
- [42] F. Kh. Abdullaev and R. M. Galimzyanov, Optical solitons in periodically managed \mathcal{PT} -symmetric media, *Optik* **157**, 353-359 (2018).
- [43] Z. Yan, Integrable \mathcal{PT} -symmetric local and nonlocal vector nonlinear Schrödinger equations: A unified two-parameter model, *Appl. Math. Lett.* **47**, 61-68 (2015).
- [44] Z. Yan, Nonlocal general vector nonlinear Schrödinger equations: integrability, \mathcal{PT} symmetry, and solutions, *Appl. Math. Lett.* **62**, 101-109 (2016).
- [45] A. Guo, G. J. Salamo, D. Duchesne, R. Morandotti, M. Volatier-Ravat, V. Aimez, G. A. Siviloglou, and D. N. Christodoulides, Observation of \mathcal{PT} -symmetry breaking in complex optical potentials, *Phys. Rev. Lett.* **103**, 093902 (2009).
- [46] C. E. Rüter, K. G. Makris, R. El-Ganainy, D. N. Christodoulides, M. Segev, and D. Kip, Observation of parity-time symmetry in optics. *Nature Phys.* **6**, 192-195 (2010).
- [47] A. Regensburger, C. Bersch, M. A. Miri, G. Onishchukov, D. N. Christodoulides, and U. Peschel, Parity-time synthetic photonic lattices, *Nature* **488**, 167-171 (2012).
- [48] M. Wimmer, A. Regensburger, M. A. Miri, C. Bersch, D. N. Christodoulides, and U. Peschel, Observation of optical solitons in \mathcal{PT} -symmetric lattices, *Nature Commun.* **6**, 7782 (2015).
- [49] T. Gao, E. Estrecho, K. Y. Bliokh, T. C. H. Liew, M. D. Fraser, S. Brodbeck, M. Kamp, C. Schneider, S. Höfling, Y. Yamamoto, F. Nori, Y. S. Kivshar, A. G. Truscott, R. G. Dall, and E. A. Ostrovskaya, Observation of non-Hermitian degeneracies in a chaotic exciton-polariton billiard, *Nature* **526**, 554-558 (2015).
- [50] I. Yu. Chestnov, S. S. Demirchyan, A. P. Alodjants, Y. G. Rubo, and A. V. Kavokin, Permanent Rabi oscillations in coupled exciton-photon systems with \mathcal{PT} -symmetry, *Sci. Rep.* **6**, 19551 (2016).
- [51] X.-W. Xu, Y.-X. Liu, C.-P. Sun, and Y. Li, Mechanical \mathcal{PT} symmetry in coupled optomechanical systems, *Phys. Rev. A* **92** 013852 (2015).
- [52] X. Zhu, H. Ramezani, C. Shi, J. Zhu, and X. Zhang, \mathcal{PT} -Symmetric Acoustics, *Phys. Rev. X* **4** 031042 (2014).
- [53] J. Schindler, Z. Lin, J. M. Lee, H. Ramezani, F. M. Ellis, and T. Kottos, \mathcal{PT} -symmetric electronics, *J. Phys. A: Math. Theor.* **45**, 444029 (2012).
- [54] J. M. Lee, T. Kottos, and B. Shapiro, Macroscopic magnetic structures with balanced gain and loss, *Phys. Rev. B* **91**, 094416 (2015).
- [55] A. Boudjemâa, Bose polaronic soliton-molecule and vector solitons in \mathcal{PT} -symmetric potential, *Commun. Nonlinear Sci. Numer. Simul.* **48**, 376-386 (2017).
- [56] H. Cartarius and G. Wunner, Model of a \mathcal{PT} -symmetric Bose-Einstein condensate in a δ -function double-well potential, *Phys. Rev. A* **86**, 013612 (2012).
- [57] H. Cartarius, D. Haag, D. Dast, and G. Wunner, Nonlinear Schrödinger equation for a \mathcal{PT} -symmetric delta-function double well, *J. Phys. A: Math. Theor.* **45**, 444008 (2012).
- [58] Y. He and D. Mihalache, Spatial solitons in parity-time-symmetric mixed linear-nonlinear optical lattices: recent theoretical results, *Rom. Rep. Phys.* **64**, 1243 (2012).
- [59] V. V. Konotop, J. Yang, and D. A. Zezyulin, Nonlinear waves in \mathcal{PT} -symmetric systems, *Rev. Mod. Phys.* **88**, 035002 (2016).
- [60] S. V. Suchkov, A. A. Sukhorukov, J. H. Huang, S. V. Dmitriev, C. Lee, and Y. S. Kivshar, Nonlinear switching and solitons in \mathcal{PT} -symmetric photonic systems, *Laser and Photonics Reviews* **10**, 177-213 (2016).
- [61] J. Yang, Necessity of \mathcal{PT} symmetry for soliton families in one-dimensional complex potentials, *Phys. Lett. A* **378**, 367-373 (2014).
- [62] V. V. Konotop and D. A. Zezyulin, Families of stationary modes in complex potentials, *Opt. Lett.* **39**, 5535-5538 (2014).
- [63] T. Mayteevarunyoo, B. A. Malomed, and A. Roeksabutr, A solvable model for solitons pinned to a \mathcal{PT} -symmetric dipole, *Phys. Rev. E* **88**, 022919 (2013).
- [64] D. Saadatmand, S. V. Dmitriev, D. I. Borisov, and P. G. Kevrekidis, Interaction of sine-Gordon kinks and breathers with a parity-time-symmetric defect, *Phys. Rev. E* **90**, 052902 (2014).
- [65] N. Karjanto, W. Hanif, B. A. Malomed, and H. Susanto, Interactions of bright and dark solitons with localized \mathcal{PT} -symmetric potentials, *Chaos* **25**, 023112 (2015).
- [66] D. A. Zezyulin, I. V. Barashenkov, and V. V. Konotop, Stationary through-flows in a Bose-Einstein condensate with a \mathcal{PT} -symmetric impurity, *Phys. Rev. A* **94**, 063649 (2016).
- [67] L. Devassy, C. P. Jisha, A. Alberucci, V. C. Kuriakose, Nonlinear waves in repulsive media supported by spatially localized parity-time-symmetric potentials, *Phys. Lett. A* **381**, 1955-1961 (2017).
- [68] A. S. Reyna and C. B. de Araújo, Spatial phase modulation due to quintic and septic nonlinearities in metal colloids, *Opt. Exp.* **22**, 22456-22469 (2014).
- [69] A. S. Reyna and C. B. de Araújo, Nonlinearity management of photonic composites and observation of spatial-modulation instability due to quintic nonlinearity, *Phys. Rev. A* **89**, 063803 (2014).
- [70] G. E. Astrakharchik, J. Boronat, J. Casulleras, and S. Giorgini, Beyond the Tonks-Girardeau gas: Strongly correlated regime in quasi-one-dimensional Bose gases, *Phys. Rev. Lett.* **95**, 190407 (2005).
- [71] F. Kh. Abdullaev and M. Salerno, Gap-Townes solitons and localized excitations in low-dimensional Bose-Einstein condensates in optical lattices, *Phys. Rev.* **72**, 033617 (2005).
- [72] K. D. Moll, A. L. Gaeta, and G. Fibich, Self-similar optical wave collapse: Observation of the Townes profile, *Phys. Rev. Lett.* **90**, 203902 (2003).
- [73] G. Fibich, *The Nonlinear Schrödinger Equation: Singular Solutions and Optical Collapse* (Springer: Cham, 2015).
- [74] J. Hukriede, D. Runde, and D. Kip, Fabrication and application of holographic Bragg gratings in lithium niobate channel waveguides, *J. Phys. D* **36**, R1-R16 (2003).
- [75] M. Vakhitov and A. Kolokolov, Stationary solutions of the wave equation in a medium with nonlinearity saturation, *Radiophys. and Quantum Electron.* **16**, 783 (1973).
- [76] E. A. Kuznetsov, A. M. Rubenchik, V. E. Zakharov, Soliton stability in plasmas and hydrodynamics, *Phys. Rep.* **142**, 103 (1986).
- [77] L. Bergé, Wave collapse in physics: Principles and applications to light and plasma waves, *Phys. Rep.* **303**, 259 (1998).
- [78] J. Yang, *Nonlinear Waves in Integrable and Nonintegrable Systems* (SIAM: Philadelphia, 2010).
- [79] H. Sakaguchi, B. A. Malomed, Solitons in combined lin-

- ear and nonlinear lattice potentials, Phys. Rev. A **81**, 013624 (2010).
- [80] T. I. Lakoba and J. Yang, A generalized Petviashvili iteration method for scalar and vector Hamiltonian equations with arbitrary form of nonlinearity, J. Comp. Phys. **226**, 1668 (2007).
- [81] D. K. Campbell, J. F. Schonfeld, and C. A. Wingate, Physica D **9**, 1-32 (1983).
- [82] D. K. Campbell, M. Peyrard, and P. Sodano, Kink-antikink interactions in the double sine-Gordon equation, Physica D **19**, 165-205 (1986).
- [83] J. K. Yang and Y. Tan, Fractal structure in the collision of vector solitons, Phys. Rev. Lett. **85**, 3624-3627 (2000).

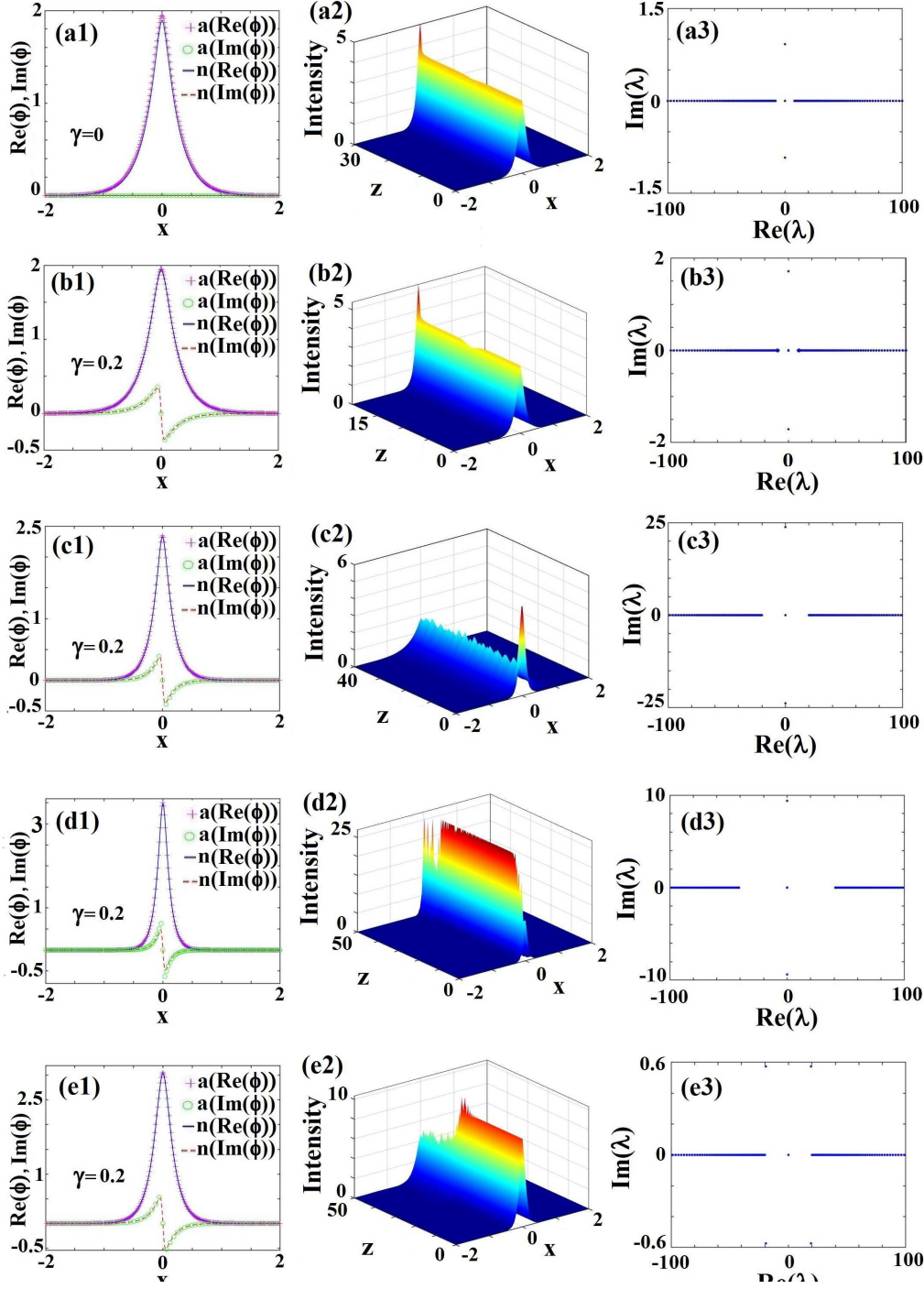


FIG. 4: (Color online). (a1), (b1), (c1), (d1), and (e1): Comparison between typical examples of unstable analytical solutions, labeled “a” (magenta pluses and green circles display their real and imaginary parts, respectively), given by Eqs. (12), (14), and (17), and their counterparts obtained from the numerical solution of Eq. (7), subject to regularization (39), labeled “n”, whose real and imaginary parts are shown by blue solid and red dashed lines, respectively. A small difference between the analytically predicted and numerically found imaginary parts of the solutions is a result of the regularization, as the analytical version is discontinuous, see Eq. (17). The simulated evolution of the numerical solutions from (a1), (b1), (c1), (d1), and (e1) is displayed, severally, in panels (a2), (b2), (c2), (d2), and (e2), and their stability spectra are depicted in (a3), (b3), (c3), (d3), and (e3), respectively. The parameters are: $\gamma = 0$, $\sigma = 2.5$, $k = 8$ in (a1, a2, a3), $\gamma = 0.2$, $\sigma = 2.5$, $k = 8$ in (b1, b2, b3), $\gamma = 0.2$, $\sigma = 2.5$, $k = 20$ in (c1, c2, c3), $\gamma = 0.2$, $\sigma = 2$, $k = 50$ in (d1, d2, d3), and $\gamma = 0.2$, $\sigma = 1.8$, $k = 20$ in (e1, e2, e3).